Advanced Studies in Pure Mathematics 43, 2006
Singularity Theory and Its Applications
pp. 55–72

The complex crystallographic groups and symmetries of J_{10}

Victor Goryunov and Show Han Man

Abstract.

We show that finite order symmetries of the function singularity J_{10} give rise to some of complex crystallographic groups listed in [12]. The groups are extracted from the equivariant monodromy of the function. This is the first appearance of affine reflection groups in a singularity context.

A series of papers [8, 9, 10, 5] has related finite order symmetries of simple function singularities to certain finite unitary reflection groups of Shephard and Todd [13]. This paper makes the next step in the same direction: we study finite order symmetries of one of Arnold's parabolic singularities [1, 3, 4], J_{10}, and construct complex crystallographic groups from the relevant monodromy.

Our approach is similar to that introduced in [8]. First of all, the cyclic group action on the homology of a two-dimensional symmetric Milnor fibre splits the homology over $\mathbb{C}$ into character subspaces H_χ. In a number of cases, as classified in [11], this splits the two-dimensional kernel K of the intersection form between two subspaces H_χ corresponding to two distinct conjugate characters: $K = K_{\chi_1} \oplus K_{\chi_2}$. In the corresponding character subspaces in the cohomology, we consider the affine hyperplanes of all 2-cocycles taking a fixed non-zero value on a fixed non-trivial element of K_{χ_i}. The equivariant monodromy on such a hyperplane turns out to be a complex crystallographic group.

Altogether our construction yields seven different affine groups. A question which naturally arises from this paper is that of existence of any version of a crystallographic group discriminant which gives hypersurfaces isomorphic to the discriminants of the symmetric J_{10} functions, similar to the relation between the discriminants of the Shephard-Todd groups and of the symmetric ADE singularities observed in [8, 9, 10].

Received March 26, 2004.
Revised August 12, 2005.
The second author was supported by an EPSRC grant.

The structure of the paper is as follows.

Section 1 introduces the affine complex reflection groups involved. Section 2 recalls, from [11], the list of symmetries of the J_{10} singularities which may lead to monodromy realisations of the groups. Here we also formulate our main result on relating the singularities and crystallographic groups. The result is then proved in Section 3. The proof is based on the consideration of the Dynkin diagrams of the symmetric singularities, which therefore may be treated as an analog of the affine diagrams of Weyl groups for the Shephard-Todd groups concerned. While the diagrams for the invariant functions have been obtained in [11], the diagram of the only equivariant function appearing is constructed in Section 4.

Finally, in Section 5, we give an example of a complex crystallographic group which is not contained in Popov's tables in [12]. This reopens Borel's problem of complete classification of complex crystallographic groups.

§1. The complex crystallographic groups

An *affine reflection* in $\mathbb{C}^n$ is an affine unitary transformation identical on a hyperplane, which is called the *mirror* of the reflection. A group generated by such reflections and having a compact fundamental domain is called *complex crystallographic*. Such groups were classified by V. L. Popov in [12].

Let $L \subset U_n$ be the linear part of a complex crystallographic group W, that is the image of W under the natural map $W \to U_n$. Of course, L must be a Shephard-Todd group. We denote by T the maximal translation subgroup of W. Then W is an extension of L by T:

$$0 \to T \to W \to L \to \{id\}$$

is an exact sequence. Unlike the real case, W may not be the semi-direct product of its linear and translation parts. However, all the groups arising in this paper from our singularity constructions are such products.

We shall now list the groups involved. Mirrors of L will be identified by their normals which we shall call *roots*.

The linear parts of the groups we will need are the Shephard-Todd groups $L = G(6,1,2)$, $G_3(6)$, G_5, G_8, G_{26}, G_{31}, G_{32}. Dynkin diagrams of these groups are given in Figure 1. The vertex set of a diagram there represents a set of generating reflections. Each vertex is a unit root and is marked with the order of the reflection, order 2 traditionally omitted. An edge $a \to b$ is equipped with the hermitian product $\langle a, b\rangle$. As usual, $\omega = e^{2\pi i/3}$. The edge orientation is omitted if the product is real, and

there is no edge at all if the roots are orthogonal. We borrow the G_{31} diagram from [10] (cf. [6]). All the other diagrams were constructed using the roots from Table 2 of [12] (see also [6]). The rank of the group G_{31} is 4. The rank of any other group is equal to the number of vertices in its diagram.

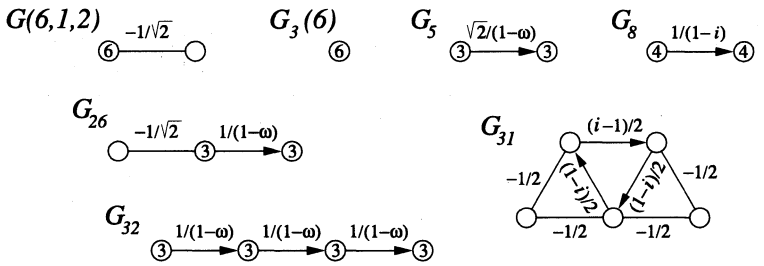

Figure 1. Dynkin diagrams of the Shephard-Todd groups. All the roots are unit.

The crystallographic group with $L = G_{26}$ arising in our situation will be shown to be Popov's $[K_{26}]_2$. Its translation subgroup T is the lattice spanned by the L-orbit of a non-zero root of any of its order 2 reflections.

The other groups will be Popov's $[G(6,1,2)]$, $[K_3(6)]$, $[K_5]$, $[K_8]$, $[K_{31}]$ and $[K_{32}]$ respectively. For each of them, the lattice T is the span of the L-orbit of any non-zero root of L. For all of these groups, except for $[K_5]$, this leaves no ambiguity in the choice since $L \neq G(6,1,2)$ is transitive on the set of its mirrors, while both obvious possibilities for $G(6,1,2)$ give the same lattice. As for $[K_5]$, when the mirror set consists of two G_5-orbits (the lattice choice between which clearly leads to the same crystallographic group), we will be a bit more specific about the preferable orbit later.

All our crystallographic groups have the conjugate versions, with i and ω replaced by their conjugates. However, the conjugations yield the same groups.

§2. Automorphisms of J_{10}

Now we introduce the singularities we will be dealing with.

Let f be a holomorphic function-germ on $(\mathbb{C}^n, 0)$. Consider a diffeomorphism-germ g of $(\mathbb{C}^n, 0)$ sending the hypersurface $f = 0$ into itself. It multiplies f by a function c not vanishing at the origin. In what follows g will have a finite order, so c is just a constant, a root of unity.

Consider the space $\mathcal{O}(g,c)$ of all holomorphic function-germs on $(\mathbb{C}^n,0)$ multiplied by c under the action of g. The group $\mathcal{R}_g$ of biholomorphism-germs of $(\mathbb{C}^n,0)$ commuting with g acts on $\mathcal{O}(g,c)$. The corresponding equivalence is a geometric equivalence in the sense of Damon [7]. Therefore, the base of an $\mathcal{R}_g$-miniversal deformation of f in $\mathcal{O}(g,c)$ is smooth and such a deformation can be constructed in the standard way [7, 4].

Definition 2.1. An automorphism g of a hypersurface $f=0$ is called *smoothable* if an $\mathcal{R}_g$-versal deformation of function f contains members with smooth zero sets.

In [11] the list of all smoothable quasihomogeneous automorphisms of all the members of the function family

$$J_{10}: x^3+ax^2y^2+xy^4, \qquad a\neq 4,$$

was obtained. Moreover, a further selection of cases with a potential to yield complex crystallographic groups was carried out in [11].

The selection was based on the construction of an affine reflection group from a semi-definite hermitian form with a one-dimensional kernel, which we briefly mentioned in the introduction. For this, we lift a smoothable automorphism of a J_{10} curve to a smoothable automorphism g of its one-variable stabilisation. As a result, the second homology of the symmetric Milnor fibre in $\mathbb{C}^3$ splits into a direct sum $\oplus_\chi H_\chi$ of character subspaces, so that g acts on an individual summand as a multiplication by the root of unity χ, $\chi^{\mathrm{order}(g)}=1$.

We want to split the 2-dimensional kernel of the J_{10} intersection form between two different H_χ. On the other hand, since we are going to extract a crystallographic group from the monodromy and since such a group has at least two generators, we need the discriminant of an $\mathcal{R}_g$-miniversal deformation of our function to be at least of multiplicity 2. Smoothable automorphisms of J_{10} satisfying these two requirements were called *interesting* in [11].

In fact, an automorphism g is used just to split the homology and does not affect any monodromy on the summands H_χ obtained. Therefore, we should not distinguish between automorphisms producing same splittings. In particular, we should not distinguish between automorphisms generating the same cyclic group. As it was shown in [11], there are just 8 different interesting symmetries of the J_{10} functions modulo such identifications. We recall them in Table 1. Notice that none of the cases contains the modulus.

The table contains seven invariant and one equivariant $(J_{10}/\mathbb{Z}_4)$ singularities. In the table, the *versal monomials* are those whose addition

with arbitrary complex coefficients to f gives an $\mathcal{R}_g$-miniversal deformation. In all the cases, their number is equal to the dimension of an H_χ on which the intersection form degenerates. The *affine groups* are those we are going to construct on such character subspaces. The *notation* of the symmetric singularities in the last column is in the spirit of that in [9]. Participation of a Weyl group in the notation (including the Weyl G_2) indicates that the discriminant of a symmetric singularity is that of the Weyl group, and hence the monodromy groups on the H_χ and the corresponding crystallographic group are in fact representations of the relevant generalised braid group, with certain powers of the generators set to be the identities.

Table 1. Symmetric J_{10} singularities

f	$g : x, y, z \mapsto$	$\lvert g\rvert$	versal monomials	kernel χ	affine group	notation
x^3 $+y^6$ $+z^2$	$\omega x, \omega y, z$	3	$1, y^3, xy^2$	$\omega, \overline{\omega}$	$[G(6,1,2)]$	$J_{10}\lvert\mathbb{Z}_3$
	$x, -\overline{\omega} y, z$	6	$1, x$	$-\omega, -\overline{\omega}$	$[K_3(6)]$	$A_2^{(6)}$
	$\omega x, -\omega y, z$	6	$1, xy^2$	$-\omega, -\overline{\omega}$	$[K_3(6)]$	$G_2^{(6)}$
	$\omega x, -y, z$	6	$1, y^2, y^4$	$-\omega, -\overline{\omega}$	$[K_5]$	$B_3^{(3,3)}$
	$x, \omega y, z$	3	$1, x, y^3, xy^3$	$\omega, \overline{\omega}$	$[K_{26}]_2$	$F_4^{(3)}$
	$\omega x, y, z$	3	$1, y, y^2, y^3, y^4$	$\omega, \overline{\omega}$	$[K_{32}]$	$A_5^{(3)}$
x^3 $+xy^4$ $+z^2$	x, iy, z	4	$1, x, y^4$	$i, -i$	$[K_8]$	$C_3^{(4)}$
	$-x, -y, iz$	4	y, y^3, y^5, x, xy^2	$i, -i$	$[K_{31}]$	$J_{10}/\mathbb{Z}_4$

Theorem 2.1. *Consider an automorphism g of a J_{10} function singularity from the table. Let H_χ be its character subspace in the second homology of a g-symmetric Milnor fibre, on which the intersection form has a non-trivial kernel. Let Γ be a hyperplane in the space dual to H_χ formed by all the*

cohomology classes taking a fixed non-zero value on a fixed element of the kernel. Let π_1 be the fundamental group of the complement to the discriminant in the base of an $\mathcal{R}_g$-versal deformation of the function. Then the monodromy group induced by π_1 on Γ is the complex crystallographic group of the table.

The proof of the theorem is given in the next section. It will use the Dynkin diagrams of the singularities for the subspaces H_χ of the table. The diagrams are given in Figure 2. Their elements represent both the degenerate intersection forms on the H_χ and the relations for the corresponding Picard-Lefschetz operators. Namely:

(1) the vertex set is a distinguished set of vanishing χ-cycles, that is of elements of H_χ which are symmetric analogues of Morse vanishing cycles (see [8, 9, 10] for details, cf. [2]);
(2) beside each vertex the self-intersection number of the χ-cycle is given;
(3) non-orthogonal χ-cycles are joined by an oriented edge labelled with the intersection number similar to how this was done for the group diagrams;
(4) however, the edge orientation is omitted in all the tree diagrams since the χ-cycles are defined up to multiplication by powers of χ and up to a choice of their own orientation (for the same reason each tree diagram serves both conjugate values of χ);
(5) inside each vertex the order of the corresponding Picard-Lefschetz operator is written (order 2 omitted);
(6) the multiplicity of an edge between vertices a and b illustrates the length of the braiding relation between the Picard-Lefschetz operators:
    - commutativity if there is no edge;
    - $h_a h_b h_a = h_b h_a h_b$ if the edge is simple;
    - $(h_a h_b)^2 = (h_b h_a)^2$ for a double edge;
    - $(h_a h_b)^3 = (h_b h_a)^3$ if the edge is triple.

In relation to Theorem 2.1, the Picard-Lefschetz operators will yield the generating affine reflections of the crystallographic groups.

The "skeleton" of a diagram with a Weyl group in the notation is the Dynkin diagram of the Weyl group. This reflects the fact that the discriminant of the symmetric singularity is isomorphic to that of the Weyl group.

For all the invariant cases, the diagrams of Figure 2 were constructed in [11] following the methods of [8, 9, 10] in a very straightforward way. The $J_{10}/\mathbb{Z}_4$ diagram will be obtained in Section 4.

Remark 2.1. The only difference between two character subspaces H_χ for each of the singularities with tree diagrams comes out in the actual Picard-Lefschetz operators. Each of them is a transformation

$$h_a : c \mapsto c - (1-\lambda)\langle c, a\rangle a/\langle a, a\rangle \tag{1}$$

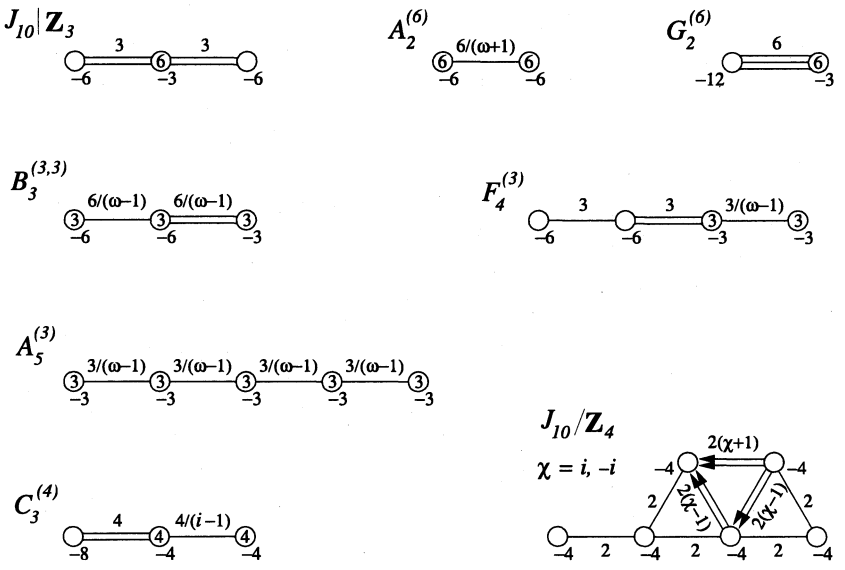

Figure 2. Dynkin diagrams of symmetric J_{10} singularities.

defined not only by its root a, but also by the eigenvalue $\lambda \neq 1$. For the operators of order greater than two, $\lambda = -\chi$ for $J_{10}|\mathbb{Z}_3$ and $B_3^{(3,3)}$, and $\lambda = \chi$ otherwise. Since the characters come in conjugate pairs, this means that the realisations of the crystallographic groups come in conjugate pairs too.

Definition 2.2. If the hermitian form $\langle \cdot, \cdot \rangle$ has a one-dimensional kernel, a transformation (1) will be called a *pseudo-reflection* provided a is not in the kernel.

Remark 2.2. The diagrams $G_2^{(6)}$ and $B_3^{(3,3)}$ are the results of folding of the diagrams $J_{10}|\mathbb{Z}_3$ and $A_5^{(3)}$ in two, similar to how the B_k diagram can be obtained from that of A_{2k-1} (see [2], cf. [8, 9, 10]). This corresponds to the symmetry groups of the second pair of singularities being index two subgroups in the symmetry groups of the first pair.

§3. Proof of Theorem 2.1

We start with some general considerations and then apply their results in a case-by-case study.

3.1. Hermitian forms of corank 1

Let $e_0, e_1, \ldots, e_k$ be coordinate vectors in $\mathbb{C}^{k+1}$. Consider a semi-definite hermitian form $\widetilde{q}$ on $\mathbb{C}^{k+1}$ with a one-dimensional kernel K spanned by $\widetilde{\mathbf{a}} = e_0 + a_1 e_1 + \cdots + a_k e_k$, where not all of the constants a_j are zero. In the basis $\{e_j\}$, the form is given by the matrix

$$\widetilde{Q} = (\widetilde{q}_{ij}) = (\widetilde{q}(e_i, e_j)) = \begin{pmatrix} \widetilde{q}_{00} & \overline{Q}_0^T \\ Q_0 & Q \end{pmatrix}$$

where Q is a $k \times k$ non-degenerate Hermitian matrix, $\widetilde{q}_{00} = \widetilde{q}(e_0, e_0)$ and Q_0 is the column of products of the $e_{i>0}$ with e_0. From the form of the kernel we see that

$$Q_0 = -Q\,\overline{\mathbf{a}} \qquad \text{and} \qquad \widetilde{q}_{00} = \mathbf{a}^T Q\,\overline{\mathbf{a}}$$

where $\mathbf{a} = (a_1, \ldots, a_k)^T$ is the *truncated kernel vector*. Matrix Q is actually the matrix of the non-degenerate hermitian form q induced by $\widetilde{q}$ on $\mathbb{C}^{k+1}/K \simeq \mathbb{C}^k$ and written in the basis formed by the projections of the $e_{j>0}$.

Assume that for each of the basic vectors e_j we have a pseudo-reflection on $\mathbb{C}^{k+1}$ with the eigenvalue $\lambda_j \neq 1$:

$$\widetilde{h}_j : c \mapsto c - (1 - \lambda_j)\frac{\widetilde{q}(c, e_j)}{\widetilde{q}(e_j, e_j)} e_j \,.$$

The matrix of the transformation $\widetilde{h}_0$ in our basis is

$$\begin{pmatrix} \lambda_0 & -\beta_0 Q_0^T \\ 0 & I_k \end{pmatrix}, \qquad \text{where} \quad \beta_0 = (1 - \lambda_0)/\widetilde{q}_{00} \,.$$

The matrices of the other $\widetilde{h}_j$ are similarly constructed from the columns of $\widetilde{Q}$ and differ from I_{k+1} in the jth rows only. The pseudo-reflections $\widetilde{h}_{j>0}$ project to $\mathbb{C}^{k+1}/K$ to the reflections h_j preserving the form q there.

Since all the $\widetilde{h}_j$ fix K, in the dual space $\mathbb{C}^{k+1,*}$ of linear functionals on $\mathbb{C}^{k+1}$, the dual operators $\widetilde{h}_j^*$ send each hypersurface formed by all the functionals taking a fixed value on $\widetilde{\mathbf{a}} \in K$ into itself.

Take one of such hyperplanes,

$$\Gamma = \{\alpha_0 + \alpha_1 a_1 + \cdots + \alpha_k a_k = b\} \subset \mathbb{C}^{k+1,*}, \qquad b \neq 0,$$

where the α_j are the coordinates dual to those we had on $\mathbb{C}^{k+1}$. Let h_0^* be the restriction of $\widetilde{h}_0^*$ to Γ. Then, in the coordinates $\boldsymbol{\alpha} = (\alpha_1, \ldots, \alpha_k)^T$ on Γ we have

$$h_0^*(\boldsymbol{\alpha}) = \begin{pmatrix} -\beta_0 Q_0 & I_k \end{pmatrix} \begin{pmatrix} b - \mathbf{a}^T\boldsymbol{\alpha} \\ \boldsymbol{\alpha} \end{pmatrix} = A_0^T \boldsymbol{\alpha} - \beta_0 b\, Q_0$$

where $A_0^T = I_k + \beta_0 Q_0\, \mathbf{a}^T$.

All the $h^*_{j>0}$ are homogeneous in $\boldsymbol{\alpha}$ and their matrices A_j^T are obtained by deleting the first row and first column of the $\widetilde{h}_j$ matrices and then taking the transposes. The deletion here means passing to the matrices of the h_j, and since these reflections preserve the form q, we have

$$A_j^T Q \overline{A}_j = Q \qquad \Longrightarrow \qquad \overline{Q}^{-1} = (A_j^T)^T \overline{Q}^{-1} (\overline{A_j^T}) .$$

Thus, the reflections $h^*_{j>0}$ preserve the hermitian form $\boldsymbol{\alpha}^T \overline{Q}^{-1} \overline{\boldsymbol{\alpha}}$ on Γ. It is easily checked that the same is true for the linear part A_0^T of h_0^* and that, moreover, the translation vector of h_0^* is a λ_0-eigenvector of A_0^T. Therefore, h_0^* is indeed an affine reflection.

Let us now pass to the coordinates $\boldsymbol{\alpha}' = Q^{-1}\boldsymbol{\alpha}$ on Γ. Then

$$\boldsymbol{\alpha}^T \overline{Q}^{-1} \overline{\boldsymbol{\alpha}} = \boldsymbol{\alpha}'^T \overline{Q} \overline{\boldsymbol{\alpha}}' \qquad \text{and} \qquad h_0^*(\boldsymbol{\alpha}') = Q^{-1}(A_0^T Q \boldsymbol{\alpha}' - \beta_0 b Q_0) = \overline{A}_0^{-1} \boldsymbol{\alpha}' + \beta_0 b \overline{\mathbf{a}} .$$

Similarly, the matrices of all the other reflections become the $\overline{A}_j^{-1}$ now. Thus, in the coordinates $\boldsymbol{\alpha}'$, we have ended up with reflections (one of them, h_0^*, affine) preserving the hermitian form with the matrix $\overline{Q}$.

Conclusion. Omit the leftmost vertex from each singularity diagram of Figure 2. It is easy to see that the subdiagrams obtained produce on the H_χ involved the monodromy groups coinciding with the linear parts L of the crystallographic groups of Section 1. Indeed orienting all non-oriented edges from the left to the right, changing the sign of the hermitian form (this move does not affect any reflections) and dividing the roots by positive numbers to make them unit we immediately get from our subdiagrams to the diagrams of Figure 1.

The only point remaining now for a verification of Theorem 2.1 is to check that the truncated kernel vector in each case is normal to a relevant mirror of L (as in the discussion of the lattices in Section 1). We carry this out in the next subsection.

In the $[K_{31}]$ case the rank 4 group G_{31} is generated by 5 reflections, but this makes no difference in the approach.

Remark 3.1. In terms of the singularities, the vertex omission mentioned above corresponds to the adjacencies of the symmetric J_{10} functions to the symmetric ADE singularities of [8, 9, 10].

3.2. The case-by-case analysis

For all the singularities, we assume that the vertices of the diagrams of Figure 2 are ordered from the left to the right starting with 0 (for $J_{10}/\mathbb{Z}_4$ the 4-valent vertex will be number 5). The components of the truncated kernel vector $\mathbf{a}$ are ordered respectively. The markings of all non-oriented edges are understood as the intersection numbers $\widetilde{q}_{j,j+1} = \langle e_j, e_{j+1} \rangle$. The $A_{j>0}$ are the matrices of the reflections h_j on $\mathbb{C}^k$ corresponding to its basic vectors e_j. Their determinants are assumed to be -1, ω, i, $-\omega$.

The one-dimensional cases $A_2^{(6)}$ and $G_2^{(6)}$ are trivial.

Elementary calculations for the other tree diagrams give the following.

$$\begin{array}{rcccl} J_{10}|\mathbb{Z}_3: & \mathbf{a} & = & (2,1) & = A_1^3 e_2 \\ B_3^{(3,3)}: & \mathbf{a} & = & (\overline{\omega}-1,-2\overline{\omega}) & = \overline{\omega}A_1^{-1}A_2e_1 \\ C_3^{(4)}: & \mathbf{a} & = & (2,-1-i) & = (1+i)A_1^{-1}A_2e_1 \\ F_4^{(3)}: & \mathbf{a} & = & (2,3,\overline{\omega}-1) & = A_1A_2A_3^{-1}A_2e_1 \\ A_5^{(3)}: & \mathbf{a} & = & (\overline{\omega}-1,-2\overline{\omega},\overline{\omega}-\omega,\omega) & = \overline{\omega}A_1^{-1}A_2A_3A_4^{-1}A_3A_2e_1 \end{array}$$

Notice that the symmetry of the G_5 diagram is destroyed in the $B_3^{(3,3)}$ case as it was promised in Section 1 and assumed by the diagram of Figure 2: the translation lattice of this realisation of $[K_5]$ is spanned by the G_5-orbit of a multiple of e_1, not of e_2.

For $J_{10}/\mathbb{Z}_4$, $\chi = i$, we get $\mathbf{a} = (2,3,2(1-i),1-i)$. According to [13, 6], for the $e_{j>0}$ in $\mathbb{C}^4$ with the diagonal hermitian form $-\sum_{s=1}^4 |z_s|^2$ we can take

$$e_1 = (2,0,0,0)\,, \qquad e_2 = (-1,-1,-1,-1)\,, \qquad e_3 = (0,1+i,0,1+i)\,,$$

$$e_4 = (0,-1-i,1+i,0)\,, \qquad e_5 = (-1,i,-1,i)\,.$$

This gives $\mathbf{a} = (1,-1,-1,1)$ which is also a root of G_{31} [13, 6]. Passing to $\chi = -i$ conjugates $\mathbf{a}$ and the e_j settings, but gives the same affine group since the mirror set of G_{31} is sent by the conjugation into itself.

This finishes the proof of Theorem 2.1.

§4. The $J_{10}/\mathbb{Z}_4$ Dynkin diagrams

We shall now construct Dynkin diagrams for the $J_{10}/\mathbb{Z}_4$ singularity starting with the two-variable case and then passing to three variables. This involves two sets of parallel objects differing just by the absence or presence of the square of an extra variable z. In order not to repeat the definitions and settings twice, all the notations for the 3-variable case will be the same as for two variables, but with the tilde on the top. This will be slightly inconsistent with the notations used in the previous sections, but will not be confusing.

4.1. The plane curve

All through this subsection $g = -id$ will be the central symmetry of $\mathbb{C}^2$, and we shall be working with g-equivariant holomorphic functions on the plane, that is series containing monomials of odd degrees only: $f(-x,-y) = -f(x,y)$.

Starting with a g-equivariant function-germ f with an isolated singularity at the origin, we slightly deform it in a generic (but still equivariant) way to a function f_* with a smooth zero set. Localising this set in an appropriate ball as it is routinely done in singularity theory, we obtain a curve V_*, a symmetric Milnor fibre of the germ f. For a generic line in the function space, to define vanishing cycles on V_*, one naturally takes the family of

levels $f_* + \alpha\ell = 0$, where ℓ is a generic linear function on the plane and α a complex parameter. Morse 1-cycles in this family vanish in symmetric pairs, $e_1 = ge_0$. Such a pair defines vanishing χ-cycles in the character spaces of g in $H_1(V_*) = H_{\chi=1} \oplus H_{\chi=-1}$:

$$e_0 + e_1 \in H_{\chi=1} \qquad \text{and} \qquad e_0 - e_1 \in H_{\chi=-1}\,. \tag{2}$$

Now take a system of paths on $\mathbb{C}_\alpha$ starting at the origin and leading to the critical values of α. Assume they have no mutual- and self-intersections, that is the system is *distinguished*. Then the corresponding distinguished systems of vanishing χ-cycles generate the H_χ [10]. However, these cycles are no longer independent: we get too many critical values of α.

For the $J_{10}/\mathbb{Z}_4$ function, it is convenient to start with a sabirification, that is a perturbation with all critical points real and all saddles on the zero level, rather than with a complete smoothing of the zero set. So we take the one-parameter family

$$f_\alpha = x(x + y^2 + y - 1)(x - y^2 + y + 1) + \alpha y\,.$$

The zero levels for two values of α, zero and sufficiently small positive α_*, are shown in Figure 3. The point α_* will now be our base point. The level $f_{\alpha_*} = 0$ will be denoted V_*, and all the cycles will be constructed in $H_1(V_*)$.

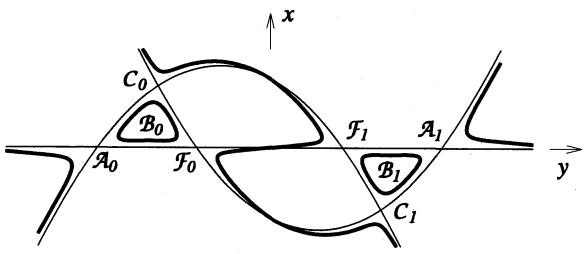

Figure 3. The curve $f_0 = 0$ (thin) and its smoothing $V_* = \{f_{\alpha_*} = 0\}$.

There are four distinct critical values of α: zero (triple), one positive (greater than α_*) and a pair of conjugates with the real part negative (see Figure 4a). The cycles vanishing on V_* along the real paths shown in Figure 4a may be traced in Figure 3. These are the $\mathcal{A}_j$, $\mathcal{C}_j$ and $\mathcal{F}_j$ vanishing at the relevant nodes of the curve $f_0 = 0$, and the ovals $\mathcal{B}_j$. The cycles vanishing along the two remaining paths will be denoted respectively $\mathcal{D}_j$ and $\mathcal{E}_j$, $j = 0, 1$. We assume that the orientations in the pairs are such that the symmetry g interchanges the cycles without affecting the orientation.

Routine calculations of the intersections yield that, within the remaining flexibility in choosing the orientations, the Dynkin diagram for the twelve 1-cycles is the one shown on the left in Figure 5.

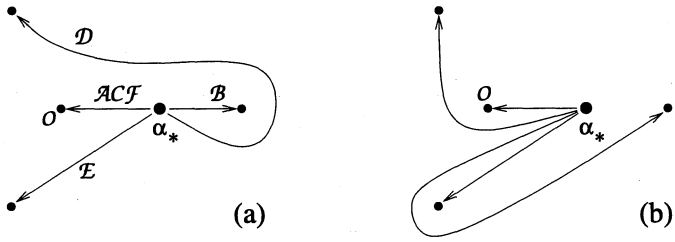

Figure 4. Distinguished path systems in $\mathbb{C}_\alpha$ leading to the critical values of the parameter α.

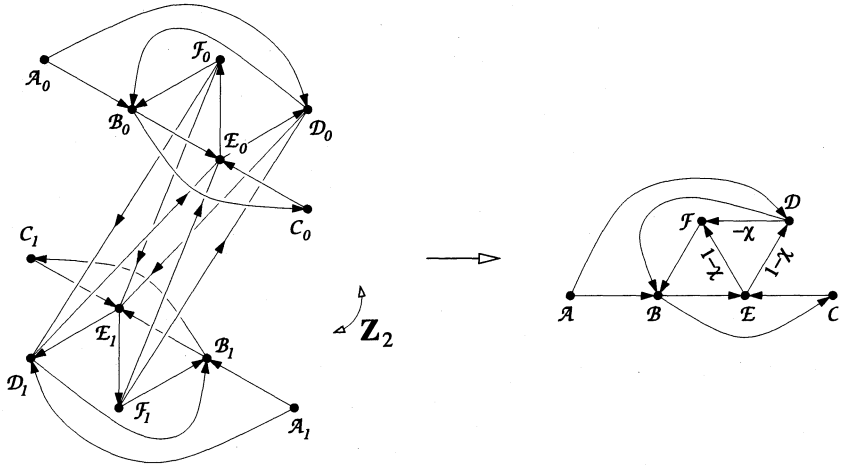

Figure 5. Folding the curve diagram to the intersection diagrams for the character subspaces $H_{\chi=\pm 1}$. On the left: an edge $a \to b$ means $\langle a, b\rangle = 1$. On the right: the label on an edge $a \to b$ is $\langle a, b\rangle/2$, with the marking 1 omitted. All the self-intersections are 0.

Passing to the intersections of the χ-cycles as in (2), we fold the 12-vertex diagram in two and obtain the diagram on the right in Figure 5.

To simplify the last diagram, we change the paths in $\mathbb{C}_\alpha$ as shown in Figure 4b. The cycles $\mathcal{B}$ and $\mathcal{D}$ are then transformed by the relevant Picard-Lefschetz operators

$$h_{\mathcal{X}} : \mathcal{Y} \mapsto \mathcal{Y} - \langle \mathcal{Y}, \mathcal{X}\rangle \mathcal{X}/2\,.$$

We also reorient the cycle $\mathcal{C}$, and multiply $\mathcal{F}$ by $-\chi$. The moves provide the diagram of Figure 6 in which the modified cycles are primed.

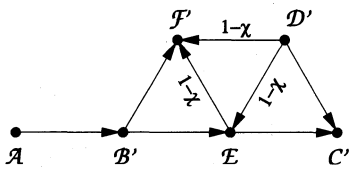

Figure 6. The Dynkin diagram for the $J_{10}/\mathbb{Z}_4$ curve corresponding to the path system of Figure 4b, $\chi = \pm 1$. The conventions are as is in Figure 5 right.

Remark 4.1. Figure 6 suggests that $\mathcal{E} - \mathcal{D}' = \mathcal{F}'$. We shall see why this is indeed the case in the next subsection.

4.2. The surface

This time we have the transformation $\widetilde{g}(x, y, z) = (-x, -y, iz)$. We restrict our attention to the functions $f(x, y) + z^2$ multiplied by $\widetilde{g}$ by -1. Morse 2-cycles of such functions vanish in symmetric pairs again, and we shall order and orient them so that

$$\widetilde{g} : \widetilde{e}_0 \mapsto \widetilde{e}_1 \mapsto -\widetilde{e}_0 .$$

Hence we have $H_2(\widetilde{V}_*, \mathbb{C}) = H_{\widetilde{\chi}=i} \oplus H_{\widetilde{\chi}=-1}$ with the summands spanned respectively by the $\widetilde{\chi}$-cycles

$$\widetilde{e}_0 - i\widetilde{e}_1 \qquad \text{and} \qquad \widetilde{e}_0 + i\widetilde{e}_1 . \tag{3}$$

For the $J_{10}/\mathbb{Z}_4$ singularity $x^3 + xy^4 + z^2$, we shall now construct the vanishing cycles on $\widetilde{V}_* = \{f_{\alpha_*} + z^2 = 0\}$ from those we obtained on V_* in the previous subsection. For this, we first recall an interpretation of the suspension of the real 1-cycle e on $x^2 + y^2 - 1 = 0$ to the real 2-cycle $\widetilde{e}$ on $x^2 + y^2 - 1 + z^2 = 0$. For this, one considers the family of levels $\phi(x, y) = \beta$ of the function $\phi = x^2 + y^2 - 1$ whose only critical value is -1. Changing β from 0 to -1, we contract the cycle e to a point and, thus, get a thimble $\tau(e)$ on the surface $\{x^2 + y^2 - 1 = \beta\} \subset \mathbb{C}^3_{xy\beta}$. Setting now $\beta = -z^2$ and taking the inverse image of $\tau(e)$ in the xyz-space we get there the 2-cycle $\widetilde{e}$.

Consider now the 2-parameter family of levels $f_0(x, y) + \alpha y = \beta$ (f_0 as in the previous subsection). Let α be close to one of its critical values α' of Subsection 4.1. Consider a Morse 1-cycle c which has nearly vanished on the level $f_0(x, y) + \alpha y = 0$. It is the boundary of the thimble $\tau(c) \subset \{f_0(x, y) + \alpha y = \beta\} \subset \mathbb{C}^3_{x,y,\beta}$ that contracts c to the nearby critical value β' of f_α along the straight path γ from 0 to β' in $\mathbb{C}_\beta$. Let us now move α along the path in $\mathbb{C}_\alpha$ from α' to α_*. This deforms γ to a path in $\mathbb{C}_\beta$ from the origin to

the relevant critical value of f_{α_*}. Respectively the thimble $\tau(c)$ becomes the thimble that contracts the cycle c (now brought to V_*) along the new path. Setting $\beta = -z^2$ doubles the new thimble and makes it into a 2-cycle in $\widetilde{V}_*$.

Applying this procedure to each of our twelve 1-cycles, we obtain twelve 2-cycles in $\widetilde{V}_{\alpha_*}$ defined by their equators in V_{α_*} and by paths in $\mathbb{C}_\beta$ leading from the origin to the critical values of f_{α_*}. To make the calculations easier, we better have the paths without mutual- and self-intersections. However, two pairs of the paths must share the same final points as there are just ten critical values. And of course the paths corresponding to a pair of g-symmetric 1-cycles should be centrally symmetric in $\mathbb{C}_\beta$.

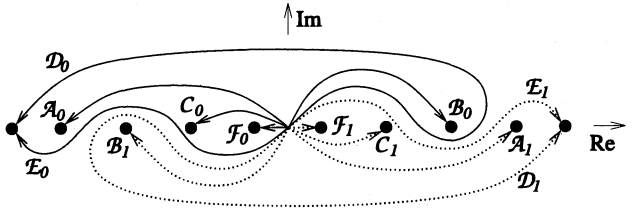

Figure 7. A path system in $\mathbb{C}_\beta$ contracting the cycles on V_* to the critical points of the function f_{α_*}.

A path system in $\mathbb{C}_\beta$ corresponding to the path system of Figure 4a and satisfying all these conditions is shown in Figure 7. To orient the resulting 2-cycles, we first orient the inverse images in $\mathbb{C}_z$ of the paths in $\mathbb{C}_\beta$. The z-paths corresponding to the $\mathcal{X}_0$ will be oriented at the origin by the tangent vectors with the positive real parts, and those for the $\mathcal{X}_1$ by the vectors with the positive imaginary parts. We orient the 2-cycle $\widetilde{\mathcal{X}}_j$ along its equator $\mathcal{X}_j$ by the orientation of $\mathcal{X}_j$ followed by the chosen orientation $z_{\mathcal{X}_j}$ of the z-path. Then

$$\langle \widetilde{a}, \widetilde{b} \rangle = -\langle a, b \rangle \cdot sgn(z_a, z_b)$$

if the two cycles meet only at the equators.

The result of the construction is the Dynkin diagram on the left in Figure 8.

The only intersection numbers in Figure 8 which still need explanation are the $\langle \widetilde{D}_j, \widetilde{E}_j \rangle$ since the cycles meet not just at the equators but at the poles too. To obtain these intersections, we notice that the path system of Figure 7 demonstrates that, in terms of the monodromy operators, the 1-cycles of the 2-variable case satisfy the relations

$$\mathcal{E}_j = h_{\mathcal{F}_j} h_{\mathcal{C}_j} h_{\mathcal{A}_j} h_{\mathcal{B}_j}(\mathcal{D}_j) = \mathcal{D}_j - \mathcal{B}_j + \mathcal{C}_j - \mathcal{F}_j \,. \tag{4}$$

The fact that the sign of $\mathcal{E}_j$ here is plus rather than minus can be easily checked by comparing appropriate intersection numbers. Relations (4), in particular,

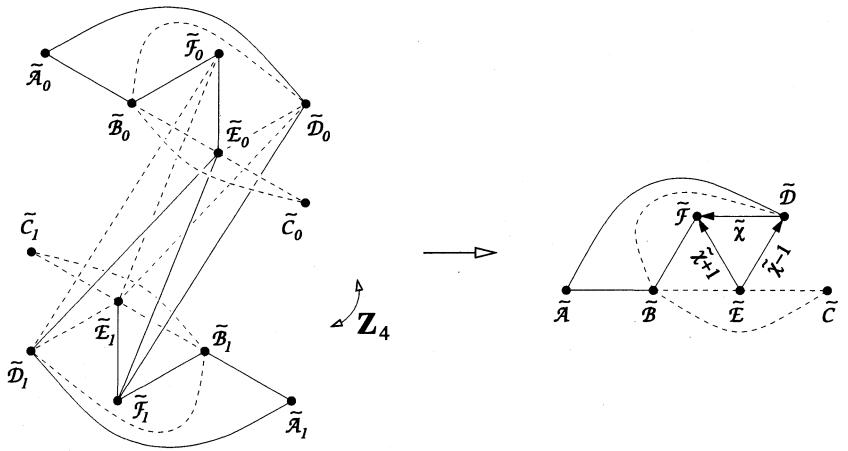

Figure 8. Folding the surface diagram to the intersection diagrams for the character subspaces $H_{\widetilde{\chi}=\pm i}$. On the left: each cycle has the self-intersection -2, a simple (dashed) edge denotes the intersection number 1 (respectively -1). On the right: the self-intersections are -4, the label on an edge is half the intersection number, marking 1 is omitted and marking -1 is presented by a dashed edge.

imply the relation of Remark 4.1. Moreover, from the same figure, we see that the same relations, but with the tildes added everywhere, hold for the 2-cycles we are considering now (the sign choice on the left can be verified like before). This gives us the numbers $\langle \widetilde{D}_j, \widetilde{E}_j \rangle$.

To get the Dynkin diagrams for the homology $H_{\widetilde{\chi}=\pm i}$, we follow the settings of (3) and fold the 12-vertex diagram in two to the diagram on the right in Figure 8, $\widetilde{\chi} = \pm i$.

Switching to the path system of Figure 4b, that is applying appropriate Picard-Lefschetz operators

$$\widetilde{h}_{\widetilde{\mathcal{X}}} : \widetilde{\mathcal{Y}} \mapsto \widetilde{\mathcal{Y}} + \langle \widetilde{\mathcal{Y}}, \widetilde{\mathcal{X}} \rangle \widetilde{\mathcal{X}}/2\,,$$

and introducing $\widetilde{\mathcal{F}}' = -\widetilde{\chi}\widetilde{\mathcal{F}}$ and $\widetilde{C}' = -\widetilde{C}$ afterwards, we end up with the diagram of Figure 9. Bearing in mind the notational difference, we see that the result is exactly the $J_{10}/\mathbb{Z}_4$ diagram of Figure 2, $\widetilde{\chi} = \chi = \pm i$. Relations (4) yield $\widetilde{\mathcal{E}} - \widetilde{\mathcal{D}} = \widetilde{\mathcal{F}}'$.

This finishes the construction.

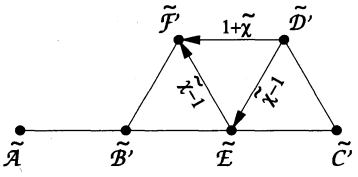

Figure 9. The Dynkin diagram for the $J_{10}/\mathbb{Z}_4$ surface corresponding to the path system of Figure 4b, $\tilde{\chi} = \pm i$. The conventions are as in Figure 8 right.

Remark 4.2. As usual, one can order the paths of Figure 4 anticlockwise in the order they leave the base point. This provides the Dynkin diagrams of Figures 6 and 9 with a standard ordering of the vertices: $\mathcal{AC}'\mathcal{F}'\mathcal{D}'\mathcal{B}'\mathcal{E}$ and the same with the tildes.

§5. An extra complex crystallographic group

This group came to our attention when the order of the Picard-Lefschetz operator corresponding to the central vertex of the $J_{10}|\mathbb{Z}_3$ diagram in Figure 2 was mistakenly taken to be 3 in [11] and the constructions of Section 3 were applied to that diagram. The rank 2 group obtained turned out to be complex crystallographic, but not contained in Popov's classification tables in [12]. We describe it now. In the spirit of Popov's notations, the group will be denoted $[G(6,2,2)]^*$.

We start with the Shephard-Todd group $G(3,1,2)$. It acts on $\mathbb{C}^2$, equipped with the hermitian form $|z_1|^2 + |z_2|^2$, by multiplying either coordinate by ω and by swapping z_1 and z_2. Therefore, it is generated by the order 3 reflection r_1 defined by the root u_1 and by the order two reflection r_2 corresponding to the root $u_2 - u_1$ (the u_j are the unit coordinate vectors in $\mathbb{C}^2$).

The group $[G(6,2,2)]^*$ is the result of the addition to $G(3,1,2)$ of the affine reflection

$$r_0 : (z_1, z_2) \mapsto (-z_2, -z_1) + (1,1)\,.$$

The reflection has root $u_1 + u_2$. Therefore, the linear part of the new group is $G(6,2,2)$ [13, 6, 10]. We shall see that the group itself is not a semi-direct product of its linear part and the translation lattice T.

Let us find the maximal translation subgroup T of $[G(6,2,2)]^*$. For this, it will be more convenient to use the transformation

$$R_0 = r_2 r_0 : (z_1, z_2) \mapsto (-z_1, -z_2) + (1,1)\,.$$

instead of r_0. Since R_0 is of order 2, any element of $[G(6,2,2)]^*$ is of the form

$$\phi = a_s R_0 a_{s-1} R_0 \dots R_0 a_2 R_0 a_1\,, \qquad a_1, \dots, a_s \in G(3,1,2)\,,$$

where a_s and a_1 may be the identity. The linear part of ϕ is $(-1)^{s-1}a_s \dots a_1$. Since $-id \notin G(3,1,2)$, for ϕ to be a translation we need $s = 2k+1$ and $a_{2k+1} = (a_{2k} \dots a_1)^{-1}$. Setting $b_j = a_j a_{j-1} \dots a_1$ so that $a_j = b_j b_{j-1}^{-1}$, we get

$$\phi = (b_{2k+1}^{-1} R_0 b_{2k+1} b_{2k}^{-1} R_0 b_{2k})(b_{2k-1}^{-1} R_0 b_{2k-1} b_{2k-2}^{-1} R_0 b_{2k-2}) \dots (b_2^{-1} R_0 b_2 b_1^{-1} R_0 b_1)\,.$$

Hence the lattice T is spanned by the translations of the form $b_2^{-1} R_0 b_2 b_1^{-1} R_0 b_1$, $b_1, b_2 \in G(3,1,2)$. These are translations by the vectors

$$b_2^{-1} R_0 b_2 b_1^{-1} R_0 b_1(0) = b_2^{-1}(t) - b_1^{-1}(t)\,, \qquad t = u_1 + u_2\,.$$

Since the $G(3,1,2)$-orbit of the vector $t = (1,1)$ consists of the nine vectors whose coordinates are 1, ω and $\overline{\omega}$, this gives

$$T = (1-\omega)\mathbb{Z}[u_1, \omega u_1, u_2, \omega u_2]\,. \tag{5}$$

Let us check that $[G(6,2,2)]^*$ has a compact fundamental domain. First of all we notice that the semi-direct product W of $G(3,1,2)$ with the lattice T of (5) is a realisation of the crystallographic group $[G(3,1,2)]_1$ of [12]. On the other hand, let W' be a similar realisation of $[G(3,1,2)]_1$, but with the finer lattice $\mathbb{Z}[u_1, \omega u_1, u_2, \omega u_2]$. Denote by W'' the group generated by W' and $-id$. Since

$$W \subset [G(6,2,2)]^* \subset W''$$

and the two groups on the sides have compact fundamental domains, the same holds for the group in the middle.

References

[1] V. I. Arnold, Critical points of smooth functions, and their normal forms, Russian Math. Surveys, **30** (1975), 1–75.

[2] V. I. Arnold, Critical points of functions on a manifold with boundary, the simple Lie groups B_k, C_k and F_4, and singularities of evolutes, Russian Math. Surveys, **33** (1978), 99–116.

[3] V. I. Arnold, S. M. Gusein-Zade and A. N. Varchenko, Singularities of Differentiable maps. Vol. I, Monographs in Mathematics, **82**, Birkhäuser, Boston, 1985.

[4] V. I. Arnold, V. V. Goryunov, O. V. Lyashko and V. A. Vassiliev, Singularities I. Local and global theory, Encyclopaedia of Mathematical Sciences, **6**, Dynamical Systems VI, Springer Verlag, Berlin a.o., 1993.

[5] C. E. Baines, Topics in functions with symmetry, PhD thesis, University of Liverpool, 2000.

[6] A. M. Cohen, Finite complex reflection groups, Annales Scientifiques de l' École Normale Supérieure, **4** (1976), 379–436.

[7] J. N. Damon, The unfolding and determinacy theorems for subgroups of $\mathcal{A}$ and $\mathcal{K}$, Memoir Amer. Math. Soc., **50**, 1984.

[8] V. V. Goryunov, Unitary reflection groups associated with singularities of functions with cyclic symmetry, Russian Math. Surveys, **54** (1999), 873–893.

[9] V. V. Goryunov, Unitary reflection groups and automorphisms of simple hypersurface singularities, New Developments in Singularity Theory, Kluwer Academic Publishers, 2001, 305–328.

[10] V. V. Goryunov and C. E. Baines, Cyclically equivariant function singularities and unitary reflection groups $G(2m, 2, n), G_9, G_{31}$, St. Petersburg Math. J., **11** (2000), 761–774.

[11] S. H. Man, Finite order symmetries of J_{10}, Banach Center Publications, **62**, Geometry and Topology of Caustics – Caustics '02, Warszawa 2004, 197–207.

[12] V. L. Popov, Discrete complex reflection groups, Commun. Math. Inst., Rijksuniv. Utr. 15–1982, 1982, 89 pp.

[13] G. C. Shephard and J. A. Todd, Finite unitary reflection groups, Canad. J. Math., **6** (1954), 274–304.

Department of Mathematical Sciences
University of Liverpool
Liverpool L69 7ZL
United Kingdom